JOURNAL OF AGRICULTURAL AND FOOD CHEMISTRY

Degradation and Persistence of Rotenone in Soils and Influence of Temperature Variations

IVANA CAVOSKI,*,† PIERLUIGI CABONI,‡ GIORGIA SARAIS,‡ AND TEODORO MIANO§

Istituto Agronomico Mediterraneo di Bari-CIHEAM, Via Ceglie 9, 70010 Valenzano, Italy, Dipartimento di Tossicologia, Università di Cagliari, Via Ospedale 72, 09124 Cagliari, Italy, and Dipartimento di Biologia e Chimica Agroforestale ed Ambientale, Università degli Studi di Bari, Via Amendola 165/A, 70126 Bari, Italy

The persistence and degradation of rotenone and its primary degradation product 12aβ-hydroxyrotenone in soils were determined under standardized laboratory conditions in the dark at 20 or 10 °C and at 40% of water holding capacity. Degradation experiments were carried out on two types of soil collected in southern Italy, a silt clay loam (SCL) and a loamy soil (L). A kinetic model was developed to describe degradation rates of rotenone, taking into account the production, retention, and degradation of the main metabolites. The DT_{50} values of rotenone and 12aβ-hydroxyrotenone, were 8 and 52 days in SCL soil, and 5 and 23 days in L soil at 20 °C, respectively. However, at 10 °C a tendency for slower degradation of rotenone and 12aβ-hydroxyrotenone was observed (25 and 118 days in SCL and 21 and 35 days in L soils, respectively). The differences were significant for most data sets. Temperature had a strong effect on degradation; a 10 °C increase in temperature resulted in a decrease in the DT_{50} value by a factor of 3.1 and 2.2 in SCL and of 4.2 and 1.4 in L soils for both rotenone and 12aβ-hydroxyrotenone, respectively. Results show that the degradation rates of both rotenone and 12aβ-hydroxyrotenone were greatly affected by temperature changes and soil physicochemical properties. The degradation reaction fits the two compartment or the multiple compartment model pathways better, which clearly indicates a rather complex rotenone degradation process in soils. Results provide further insights on the rates and the mechanisms of rotenone degradation in soils, aiming to more clearly describe the degradation pathway of chemical residues in the environment.

KEYWORDS: Biopesticide; chemical residues; metabolites; 12aα-hydroxyrotenone; half-life

INTRODUCTION

Soil acts like an active filter where chemical compounds are degraded by physical, chemical, and biological processes. It is also a selective filter because of its capacity to retain chemicals and avoid their seepage into aquifers (*1*). Both the accumulation of pesticides in the soil and their dispersion in the environment depend chiefly on the characteristics and overall functioning of the ecosystem. Soil represents a major sink for organic xenobiotic contaminants in the environment. Besides sorption, degradation is the second most important theoretical process utilized to predict the fate of pesticides in soils (*2*).

The extent to which organic chemicals are retained within the soil is controlled by the main physicochemical properties of both soils and contaminants. The persistence of a pesticide in soil depends partly on the effectiveness of transfer processes, such as evaporation, leaching, erosion, and plant uptake. Prediction or determination of pesticide degradation in soil is a significant part of the data package submitted for pesticide registration (*3*). Conversion of parent compounds does not always result in reduced biological activities of the derived byproduct. In some cases, the first conversion products may be more active than the original compound; in fact, it can be more dangerous to different living organisms. Classical examples are parathion and its metabolite paraoxon (*4*), and fipronil and its desulfinyl derivative (*5*). Therefore, a detailed knowledge of the degradation pathways as well as the rate of disappearance of the parent compounds is needed in order to clearly define the effects produced by pesticides and their degradation byproducts.

Weakly polar hydrophobic compounds (sparingly soluble in water, with a low vapor pressure and a recalcitrant molecular structure) are retained strongly within the soil (*6*). Initially, a portion of the contaminant can be sorbed quickly by the soils, whereas the remaining fraction is sorbed more slowly over

* Corresponding author. Tel: +39/080-4606-340. Fax: +39 /080-4606-262. E-mail: cavoski@iamb.it.
† Istituto Agronomico Mediterraneo di Bari-CIHEAM.
‡ Università di Cagliari.
§ Università degli Studi di Bari.

10.1021/jf801461h CCC: $40.75
Published on Web 08/06/2008

weeks or months (*7*). The initial rapid sorption is generally determined by the formation of hydrogen bonding and van der Waals forces, i.e., mechanisms that are expected to occur instantaneously upon contact of the hydrophobic organic compound with the soil surface (*8, 9*). However, sorption is generally governed by partitioning between the solution and the organic matter phases, being specific interactions (chemisorption) unlikely to affect these contaminants (*10*). The sequestration of hydrophobic organic components by soils, described by diffusion through organic matter and sorption-retarded pore diffusion, has been described in detail elsewhere (*11, 12*).

Rotenone is a botanical insecticide, with some acaricidal properties and used for fish eradication in water body management (*13*). Rotenone is a natural compound and most studies emphasize its mechanisms of toxicity (*14*), biotoxicity (*15*), and the presence of residues in various crops (*16*).

In the determination of residues on crops treated with rotenone, it is important to determine the occurrence of the major toxic decomposition product, 12α,β-hydroxyrotenone, as well as rotenone. The LD_{50} values are 7.2 and 8.0 mg kg^{-1} for 6′,7′-epoxy-rotenone and O-demethylrotenone, respectively, vs 2.8 mg kg^{-1} for rotenone (*17*), whereas the reported value for rotenolones I (12aβ-hydroxyrotenone combined with some 12aα-hydroxyrotenone) is 4.1 mg kg^{-1} (*18*).

Rotenone is susceptible to microbial degradation; microbial enzymes catalyze the introduction of a molecule of oxygen into the isopropylene side-chain of rotenone forming 1′,2′-dihydrorotenone (*19*). Sariaslani and coauthors described the production, isolation, and identification of 12aβ-hydroxyrotenone as the major product formed by the oxidation of rotenone by laccases, enzyme of the *Ascomycetes*, *Basidiomycetes*, and the *Fungi Imperfecti* (*20*).

Although rotenone has been a commercial product for many years, there are no reported studies on its residues in the soil. In experiments carried out to study photodegradation of rotenone in soils under environmental conditions, the observed overall degradation of rotenone is not only determined by photolysis itself but also as a function of soil characteristics, and it appears to be reduced and affected by several other physical−chemical mechanisms (*21*). To completely evaluate the environmental hazard of rotenone, it is necessary to establish the ultimate fate of the parent compound and its degradation products in the soil. The aim of this study is to provide more detailed knowledge about the pathway, rate, and mechanism of degradation for rotenone as well as its metabolites in soils.

MATERIALS AND METHODS

Materials. Acetonitrile and acetone (HPLC grade), and ethyl acetate (analytical grade) were purchased from BAKER (Mallinckrodt Baker, Holland). Ultra pure water was obtained from the Millipore (Billerica, MA) Milli-Q system. Rotenone (purity 95 − 98%) was purchased from Sigma Aldrich (Steinheim, Germany), whereas standards of rotenoids were kindly provided by Professor J. E. Casida from the University of California at Berkeley. Rotenone structure and physicochemical properties are presented in **Figure 1** and **Table 1**. A stock standard solution of rotenone (1000 mg L^{-1}) was prepared in acetone. Working standard solutions were prepared daily by dilution with the mobile phase acetonitrile/water (60:40, v/v).

HPLC/UV Determination. The HPLC system (Dionex, Germering, Germany) was equipped with an UVD 170U detector, low pressure pump P680 HPLC pump, injector with 20 μL loop, and the column Acclaim C18 reverse (150 × 4.6 mm I.D., particle size 5 μm). HPLC was controlled, and data were elaborated using Chromeleon Software (Dionex, Germering, Germany). Isocratic separation was performed with a mobile phase of acetonitrile/water (60:40, v/v) in 15 min. The injection

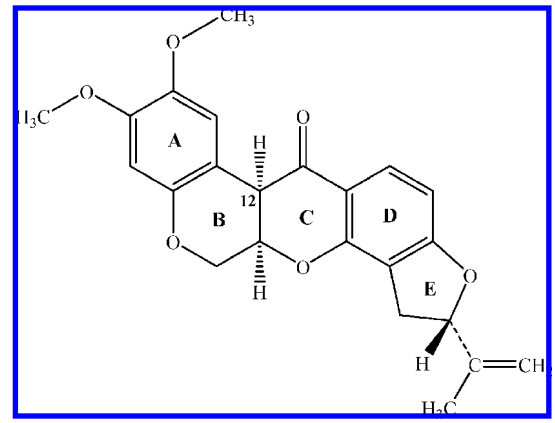

Figure 1. Rotenone structure.

Table 1. Physico-Chemical Parameters of Rotenone

parameters	value
molecular weight (g mol^{-1})	394.4 (*13*)
solubility in water (mg L^{-1})	0.2 [25 °C] (*22*)
vapor pressure (Pa)	1.3×10^{-4} (*22*)
henry's law constant (Pa m^3 mol^{-1})	<0.03 (*23*)
melting point (°C)	163−181 (*13*)
partition coefficient *n*-octanol−water: log K_{ow}	4.1 (*24*)[a]
partition coefficient organic carbon−water: log K_{oc}	4.0 (*22*)[a]

[a] Calculated.

volume was 20 μL, and the flow rate was 1 mL min^{-1}. The analysis was performed at a wavelength of 295 nm. External calibration of 0.1−10 mg L^{-1} ($R^2 = 0.999$) was used.

HPLC/ESI-MS/MS Analysis. A Varian tandem mass spectrometer (Palo Alto, CA, USA) consisting of a ProStar 410 autosampler, two ProStar 210 pumps, and a 1200 L triple quadrupole mass spectrometer equipped with an electrospray ionization source was used. Varian MS workstation, version 6.7 software was used for data acquisition and processing. Chromatographic separation was performed on an XDB column (2.1 × 250 mm I.D., particle size 5 μm, Milford, MA). The mobile phase consisted of (A) methanol and (B) bidistilled water. Elution was with methanol−water (75:25, v/v) for 16 min. The mobile phase, previously degassed with high-purity helium, was pumped at a flow rate of 0.4 mL min^{-1}, and the injection volume was 20 μL. The electrospray ionization-mass spectrometer was operated in the positive ion mode. The electrospray capillary potential was set to 35 V, while the shield was at 725 V. Nitrogen at 49 mTorr was used as a drying gas for solvent evaporation. The atmospheric pressure ionization (API) housing and drying gas temperatures were kept at 50 and 380 °C, respectively. Protonated analyte molecules of the parent compounds were subjected to collision induced dissociation using argon at 3.80 mTorr in the multiple reaction monitoring (MRM) mode. The scan time was 1 s, and the detector multiplier voltage was set to 1400 V, with an isolation width of *m/z* 1.2 for quadrupole 1 and *m/z* 2.0 for quadrupole 3. Selected reaction monitoring (SRM) of the precursor−product ion transitions *m/z* 395 → 192, 395 → 213 for rotenone, and *m/z* 393 → 365 for 12aβ-hydroxyrotenone were used for quantitation.

Soil Sampling and Analysis. Two soils were sampled in two different locations: Turi (SCL) and Valenzano (L) of Puglia region (South Italy), 20 cm from the top. Geographical coordinates for SCL (*x*, 672410.6; *y*, 4531557.9) and L (*x*, 657618.8; *y*, 4546479.7) were determined by UTM (Universal Transverse Mercator European Datum 1950). Plant macroresidual materials, macro faunal remains, and stones were accurately removed, and larger soil aggregates were manually and gently fragmented into smaller ones, prior to the subsequent fractionation procedure. Soils were air-dried and sieved < 2 mm. Soil analyses were carried out following internationally recommended procedures and official methods (*25*). Soil physical and chemical properties are shown in **Table 2**. Soils were stored at 4 °C for a week; before starting degradation tests, soils were preincubated to reach 40% whc (water holding capacity) and re-establish equilibrium.

Table 2. Physico-Chemical Properties of Selected Soils[a]

parameters	L	SCL
$pH_{1:2.5}(H_2O)$	8.6	7.7
$pH_{1:2.5}(KCl)$	7.7	6.8
$EC_{1:2}(dS\ m^{-1})$	0.13	0.24
clay (g kg^{-1})	244	363
silt (g kg^{-1})	335	524
sand (g kg^{-1})	421	113
texture USDA	loam	silt clay loam
−33 kPa water content (g water/100 g dry soil)	19	29
CEC $cmol_{(+)}kg^{-1}$	10.6	21.1
OC (g kg^{-1})	7.1	28.9
N total (g kg^{-1})	0.7	3.1
C/N	9.5	9.6

[a] L, loam; SCL, silt clay loam; EC, electrical conductivity; CEC, cation exchange capacity; OC, organic carbon.

Experimental Setup. The soils used in this experiment were soil type SCL and L; these soils were selected because of their marked differences in physicochemical characteristics (**Table 2**). Soils were spiked with 2.5 mL of 5000 mg L^{-1} rotenone solution in acetone to reach a concentration of 10 mg kg^{-1} in 500 g of dry soil. The final concentration of acetone was less than 0.5% (v/w). Then, the soils were thoroughly mixed with a spatula and left in the dark till solvent evaporation. One gram soil aliquots were used to check the uniform distribution of rotenone (recovery of 5 replicates was 94 ± 4%). The initial concentration does not correspond to the level of applied rotenone in the upper 10 cm of the soil, if the maximum dose is spread in one treatment. A two times higher dose was chosen in order to evaluate the worst case scenario and to follow the formation and degradation of main metabolites. Soils were transferred into incubation flasks, which were tightly closed and reopened each two days in order to maintain aerobic conditions. The soil degradation studies were performed in standardized laboratory condition in the dark at 20 ± 2 °C and 10 ± 2 °C at 40% whc in the following treatments: SCL 10 (soil type SCL at 10 °C); SCL 20 (soil type SCL at 20 °C); L 10 (soil type L at 10 °C); and L 20 (soil type L at 20 °C). The incubation flasks were weighed, capped, and transferred to incubators at the required temperatures. The moisture was controlled every single week by weighing the incubation flasks and by resupplying water losses by adding distilled water if necessary. Furthermore, untreated soil samples were incubated under the same conditions. Time intervals were preferred in such a way that pattern of decline of the test substance and patterns of formation and decline of transformation products can be established. Samples were taken on 14 dates (0, 4, 7, 10, 14, 21, 28, 35, 49, 63, 94, 124, 154, and 184 days) with three replicates per date following the OECD guidelines (*26*). In each series of sample analysis, the rotenone content in the soils was adjusted to water content. Then, 5 g of soil samples were placed in Pyrex glass tubes, and 10 mL of ethyl acetate was added. Samples were end-over-end mixed for 30 min. Then, the organic solvent phase was separated by centrifugation at 6500 rpm for 10 min, and 1 mL of the organic extract was transferred to a 2 mL vial under a gentle nitrogen stream till complete evaporation of the solvent. Residues were redissolved with 0.5 mL of the mobile phase and injected into the HPLC-UV for chromatographic analysis. Recovery assays were performed for rotenone and its metabolite by using standards to reach the concentrations of 0.1, 1.0, and 10.0 mg kg^{-1} in both type of soils. Mean recoveries of rotenone and rotenolone from soils ranged from 94 to 100% with coefficients of variation of 1 to 5%. Limits of detection and limits of quantification for rotenone and rotenolone were 0.01 mg kg^{-1} and 0.01 mg kg^{-1}, respectively for soils.

Curve Fitting and Statistics. The actual degradation rate was calculated for each sampling time using the ModelMaker software, version 4.0; the graphical compartmental and system dynamic modeling software package provides the best fit line for the experimental data (*27*). Two kinetic models were used to fit the degradation data of rotenone and main metabolites (*28*): (1) a simple first-order equation (exponential kinetic model) for rotenone and its metabolite (SFO-SFO) and (2) a first-order multicompartment model (*29*) for rotenone and a simple first-order equation for possible metabolites (FOMC-SFO). Model parameters were optimized according to recommendations given by FOCUS (*28*) and using the least-squares method. A fit that results in an error level of 15% is considered acceptable, although this is not an absolute cutoff criterion, and a visual assessment must be made. All data were analyzed using the General Linear Models Procedure (SAS Institute, Inc. 2001). Mean separation among lines was accomplished using the Duncan Multiple Range Test at $P < 0.05$.

RESULTS AND DISCUSSION

Degradation Product Identification. Retention time and HPLC/ESI/MS/MS fragmentation patterns were the criteria used for compound identification, using the commercially available rotenone and a standard of 12aβ-hydroxyrotenone. Rotenone gave the *m/z* 395 $[M + H]^+$ and 436 $[M + H + CH_3CN]^+$ adducts, while 12aβ-hydroxyrotenone (ROT-OH) gave the *m/z* 393 $[M + H - H_2O]^+$ adduct (*39*). For all soil extracts, rotenone and its main product of degradation, 12aβ-hydroxyrotenone (*17*), were identified and confirmed by LC/MS/MS analyses, monitoring (i) in the scan mode the ions from 340 till 425 *m/z* (**Figure 2A**) and (ii) in the MRM mode following the transitions previously reported (**Figure 2B**). LC/MS/MS retention times for rotenone and 12aβ-hydroxyrotenone were 13.85 and 11.66 min, respectively.

Another metabolite, 12aα-hydroxyrotenone, occurs in soil treatments under experimental conditions, providing the *m/z* 393 $[M + H - H_2O]^+$ adduct like 12aβ-hydroxyrotenone (monohydroxylated rotenone) but with a longer retention time of 14.79 min. Matching retention times of authentic standards with fragmentation pattern allowed the identification and quantification of rotenone and 12aβ-hydroxyrotenone. 12aα-Hydroxyrotenone was detected as rotenone metabolites in several studies (*17, 30, 31*). The chromatograms were compared with corresponding untreated soil chromatograms where no interfering peaks were detected. As shown in **Figure 2A**, in the scan mode from 340 to 425 ions *m/z*, where masses of all possible metabolites of rotenone degradation should be located, no other peaks were observed.

Formation of 12aβ-hydroxyrotenone and decline under different soils and soil treatments are shown in **Figure 3**. Initial concentration (mg kg^{-1}) of extracted 12aβ-hydroxyrotenone was 0.49 ± 0.01 for SCL 20, 0.53 ± 0.17 for SCL 10, 0.45 ± 0.21 for L 20, and 0.49 ± 0.15 for L 10 soils, reaching the maximum of 2.91 ± 0.12 after 29 days of incubation for SCL 20, 3.45 ± 0.27 after 49 days for SCL 10, 3.82 ± 0.13 for L 20 after 29 days, and 4.90 ± 0.13 for L 10 after 35 days. At the end of the experimental time, 12aβ-hydroxyrotenone decreased to 0.70 ± 0.02 in SCL 20, 2.68 ± 0.02 in SCL 10, 0.12 ± 0.01 for L 20, and 0.42 ± 0.02 in L 10. In the case of the other metabolite, 12aα-hydroxyrotenone, it was not possible to follow the kinetics of formation and decline because of its relatively small yield (below 10% in all treatments) and because of the high variability in all treatments. In fact, it is considered as a minor metabolite in the rotenone degradation pathway.

In the soil environment, chemical attacks by oxidation and hydrolysis are highly possible. The products are oxidized derivatives; therfore, oxygen plays a critical role. The principal chemical reactions of rotenone are probably initiated by abstraction of the hydrogen in the 12a position by another rotenone molecule in an excited electronic state. [Rotenone acts as a photosensitizer in other photochemical reactions (*32, 33*).] The reaction of molecular oxygen with the newly created radical intermediate then has the possibility of forming two isomeric hydroperoxide intermediates, which can decompose to the corresponding isomers hydroxyrotenones (*17*). A number of chemical processes such as hydrolysis, oxidation, and isomer-

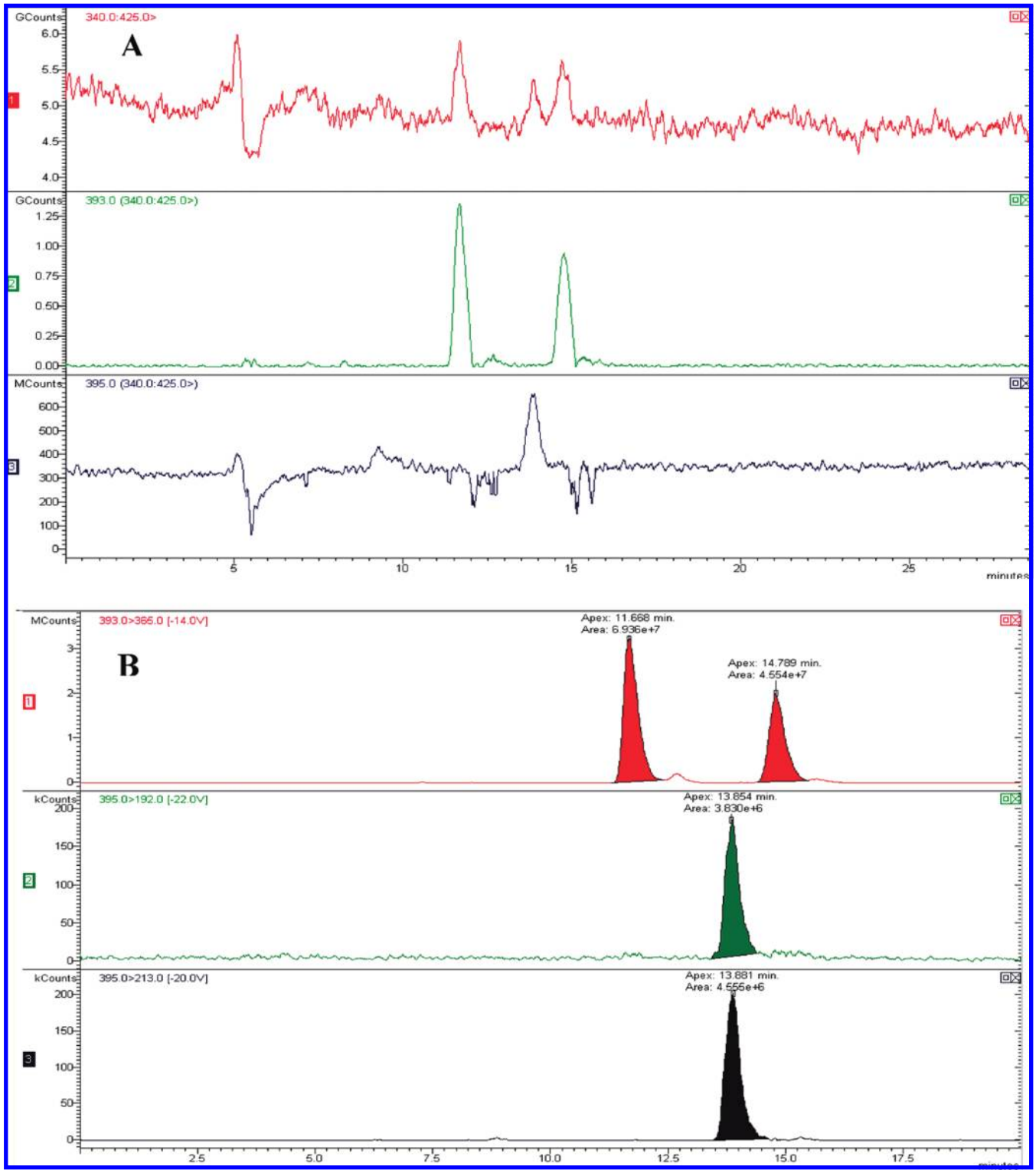

Figure 2. LC/MS/MS chromatograms of L 10 soil after 56 days of incubation in the scan mode from 340 to 425 ions *m*/*z* (**A**) and in the MRM mode (**B**).

ization are responsible for rotenone degradation in soil. The degradation of rotenone in soils produces principally an oxidized metabolite 12aβ-hydroxyrotenone and its isomer 12aα-hydroxyrotenone by hydroxylation of the 12a-position of the B−C ring (**Figure 1**).

Degradation Experiment. Degradation was analyzed using two different models as mentioned earlier. The formation rate of metabolites and the degradation rate of rotenone are directly related as they occur simultaneously, which can result in correlation with formation and degradation parameters. The conversion of concentration of metabolite presented in **Figure 3** to the percentages presented in **Figures 4** and **5** was done according to the model of kinetics applied in the presence of an amount of metabolite, practically a percentage of initial rotenone concentration. The flow of parent−rotenone to main metabolites and the current flow from parent and metabolite to further degradation products are presented in this case by minor metabolites, bound residues and CO_2.

Comparison was made on the basis of visual assessment (**Figures 4** and **5**) and χ^2 tests (**Table 3**).

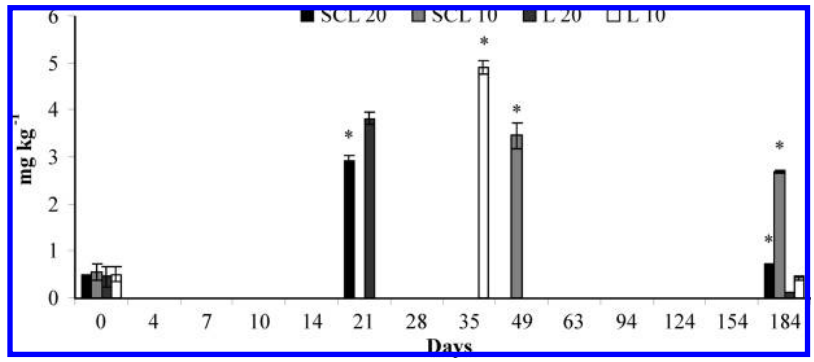

Figure 3. 12aβ-Hydroxyrotenone formation and decline in different treatments during the incubation time, *$P < 0.05$.

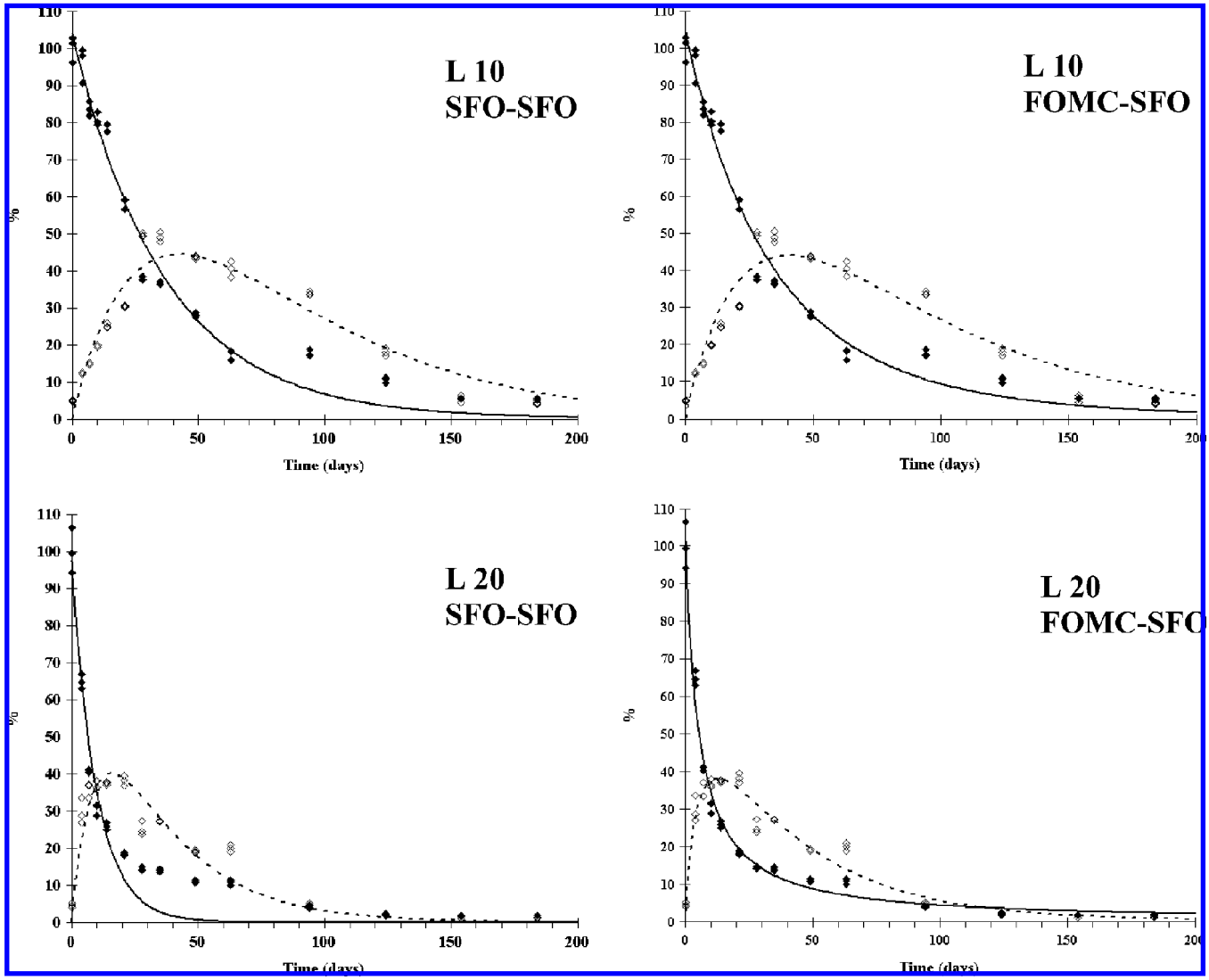

Figure 4. Experimental data of rotenone degradation (♦) and ROT-OH formation and degradation (◊) in L soil at two different temperatures. SFO and FOMC, for rotenone (—) and ROT-OH (- - -).

DT_{50} (disappearance time 50) and DT_{90} (disappearance time 90), the time within which the percentage of the test substance is reduced by 50% and 90%, and χ^2 error values are presented in **Table 3**. DT_{50}s for rotenone, varied from 5 to 8 days for L 20 and SCL 20 and from 21 to 25 days for L 10 and SCL 10, respectively. The fast degradation in the first compartment occurs when the pesticide is in the soil−water phase and readily available for degradation. In the second compartment, the pesticide is sorbed onto soil particles. Degradation is, therefore, controlled by the rate of desorption and diffusion into the soil−water phase. The partition between the two compartments depends on the pesticide sorption properties and soil characteristics. Often, the degradation does not follow simple first-order kinetics, but it shows a biphasic pattern where soil residues decrease slowly after an initial rapid decline and persist at a low level until the end of the experimental period. According to FOCUS guidance (*28*), values are considered to be acceptable, and the observed differences were significant at $P < 0.05$ according to statistical analysis. However, obtained DT_{50} values appeared to be different from previously estimated ones from

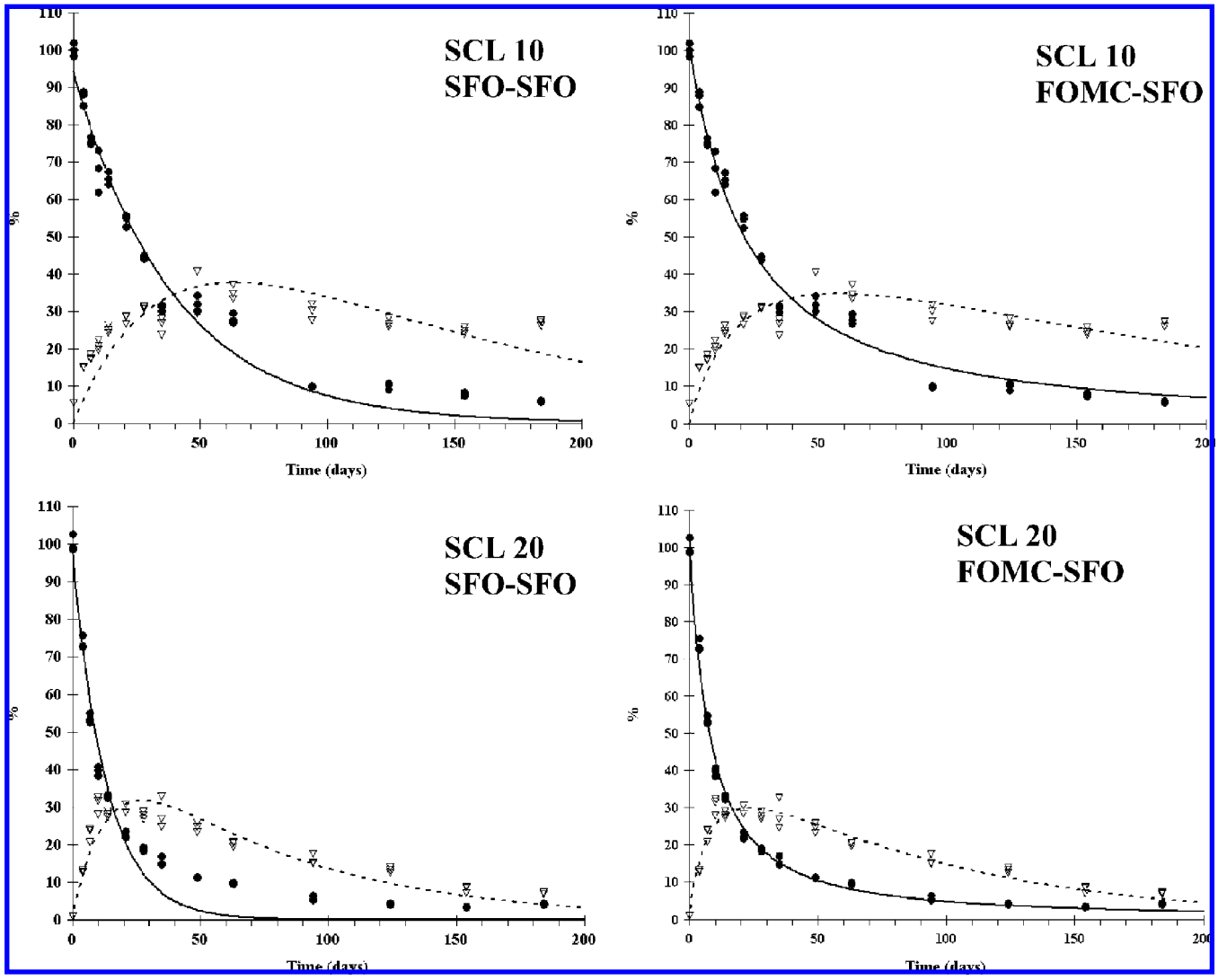

Figure 5. Experimental data of rotenone degradation (●) and ROT-OH formation and degradation (▽) in SCL soil at two different temperatures. SFO and FOMC, for rotenone (—) and ROT-OH (- - -).

Table 3. Parameters of Rotenone (R) and 12aβ Hydroxyrotenone (R-OH) Kinetics in Soils, Results of Two Pathway Models, Goodness of Fit (χ^2 Error), DT_{50}, and DT_{90} Values and Factor Q_{10}[a]

	rotenone SFO-12aβ-hydroxyrotenone SFO				rotenone FOMC −12aβ-hydroxyrotenone SFO			
parameters	L 10	L 20	SCL 10	SCL 20	L 10	L 20	SCL 10	SCL 20
K_R(d^{-1}, SFO)	0.027	0.102	0.026	0.074				
$K_{R\text{-}OH}$(d^{-1})	0.020	0.036	0.009	0.014	0.015	0.030	0.006	0.013
χ^2_R (%)	9.2	21.5	9.1	15.9	8.7	9.3	6.5	6.7
$\chi^2_{R\text{-}OH}$(%)	14.9	30.8	18.3	13.8	10.2	13.5	15.0	9.3
DT_{50R}	25	7	24	9	21	5	25	8
DT_{90R}	84	23	90	31	95	43	142	51
Q_{10R}					4.2		3.1	
$DT_{50R\text{-}OH}$	35	20	77	48	35	23	112	52
$DT_{90R\text{-}OH}$	117	65	258	159	114	77	371	172
$Q_{10R\text{-}OH}$					1.4		2.2	

[a] All data are expressed in d - days; single first order (SFO) and first order multi compartment (FOMC) percentage error levels (χ^2), the smaller the error the better the fit: errors below 15% are considered acceptable provided the visual fit is adequate (28); $K_{R;\ R\text{-}OH}$ = rate constants for R-rotenone and R-OH for 12aβ-hydroxyrotenone; DT_{50} and DT_{90} values for rotenone and 12aβ- hydroxyrotenone in soils; Q_{10}, factor by which degradation increases when temperature increases by 10 °C.

12 days (*34*). Since each data point in the degradation experiments was based on three replicates, the smoothness of the curves indicates the high reproducibility of the whole experimental procedure (**Figures 4** and **5**). DT_{50}s values varied from 23 and 52 days for L 20 and SCL 20, and 35 and 112 days for L 10 and SCL 10 for 12aβ-hydroxyrotenone, respectively. SFO-SFO kinetics provide a poor fit to the data for rotenone and 12aβ-hydroxyrotenone as shown by all experiments (**Figures 4** and **5**). The calculated curves do not very closely match the observed pattern for parent and metabolite compounds. The derived DT_{50} values of SFO-SFO for rotenone and the main metabolite may not be taken into account in regular risk assessments, although the visual agreement between observed and simulated data is relatively poor. The decline of residues is underestimated by simple first-order kinetics early after treatment and overestimated later in periods (**Figures 4** and **5**). The decline in rotenone residues (K_R) extracted with organic solvent followed the series L 20 < SCL 20 < L 10 < SCL 10, while for 12aβ-hydroxyrotenone ($K_{R\text{-}OH}$), it followed a different order: L 20 < L 10 < SCL 20 < SCL 10. The biphase FOMC models for rotenone and SFO for 12aβ-hydroxyrotenone fit the data more closely than SFO-SFO in experimental conditions (**Figures 4** and **5**). Smaller χ^2 values and better fitting of data process description were achieved in FOMC-SFO models.

A fast initial degradation of rotenone (**Figures 4** and **5**) is often followed by a slower decline, resulting in much higher

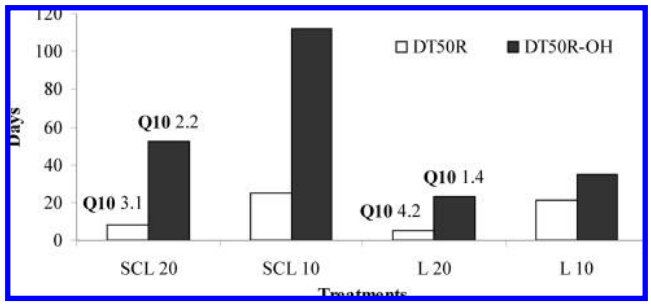

Figure 6. DT_{50R} (50% disappearance time, rotenone) and $DT_{50R\text{-}OH}$ (50% disappearance time, 12aβ-hydroxyrotenone) in different treatments with corresponding Q_{10} factors.

DT_{90}s values, varying from 43 to 51 days for L 20 and SCL 20, and 95 and 142 days for L 10 and SCL 10 for rotenone, respectively; DT_{90}s values for 12aβ-hydroxyrotenone varied from 77 and 172 days for L 20 and SCL 20, and 114 and 371 days for L 10 and SCL 10, respectively.

Rotenone degradation phenomena are clearly described by a biphasic equation, which clearly fits measured data of the molecule remaining in the soils, while 12aβ-hydroxyrotenone kinetics is described by a first order equation. In environmental studies, changes in temperature and/or moisture can affect the degradation rate and caused deviations from first order kinetics as reported in experiments regarding rotenone photodegradation on soil surfaces (*21*). Normally, as the time of contact between contaminant and soil increases, a decrease in chemical and biological availability, a process termed aging, is observed (*35*). The available fraction often decreases with time because of slow sorption and diffusion processes (*36*). Since nonpolar organic contaminants have low aqueous solubility and strong affinity for organic matter, at any time only a very small proportion of a given compound will be present in the soil solution.

Temperature Effect on Rotenone and 12aβ-Hydroxyrotenone Degradation in Soil. Rotenone degradation is temperature dependent, and soils show significantly different net loss due to the temperature variation. Temperature had a strong effect on degradation, and an increase in temperature by 10 °C (Q_{10}) resulted in a decrease in the DT_{50} values by a factor of 4.2 in soil type L and of 3.1 in soil type SCL for rotenone, and by a factor of 1.4 and 2.2 in soil types L and SCL, respectively for 12aβ-hydroxyrotenone (**Table 3** and **Figure 6**). It seems that a temperature fluctuation exerts a noticeable effect in L soil especially for rotenone degradation. Higher temperature is usually observed to promote more rapid desorption of organic contaminants from soils, and this is commonly viewed as an activated process (*37*). It is well known that soil temperature affects pesticide degradation rate, the water−air partition coefficient, and the water−soil partition coefficient. These three parameters are components of the retardation factor and attenuation factor, and contribute to the determination of pesticide behavior in the environment (*38*).

A pesticide can be found in soil, as vapor diluted in the air of the soil, and as solute diluted in the aqueous solution of the soil or adsorbed onto the organic and mineral components of the soil. Our results are widely confirmed by several other authors (*39*−*42*).

Effect of Soil Composition. The pesticide sorption characteristic and pesticide half-life in the soil describe the pesticide leaching potential and persistence in soil. The K_d values of rotenone in the adsorption experiment were 0.56 and 2.73 L kg $^{-1}$ for L and SCL soils (*43*), respectively, and the degradation rates were 0.102 and 0.074 d^{-1} for soils at 20 °C. There were some marked differences between the soils in their ability to degrade rotenone. Degradation may be influenced by adsorption onto a reactive surface. A positive relationship between sorption coefficient (K_d) and half-life has been reported for many ionizable pesticides (*44*). Assuming that only the dissolved portion of the pesticide in the soil solution is freely available to microorganisms, the rates of microbial degradation may be expected to decrease. Thus, the effect of sorption on the degradation pathway depends on many factors including soil physical and microbial characteristics and the properties of the chemical compound. The degradation rate decreases in soils where rotenone is less adsorbed. Lower availability/bioavailability of rotenone is governed by its molecular properties such as aqueous solubility and K_{OW} (**Table 1**). However, the contribution of chemical processes to the global consumption rate is higher in soils richer in organic matter than in sandy soil.

There is evidence that adsorption may also protect pesticides against chemical attack so that degradation is not possible. Microorganisms are generally more abundant onto or near soil particle surfaces (*45*). Sorption may concentrate the pesticide in regions of greater microbial activity, thereby facilitating degradation. However, pesticide is often sorbed on the walls of small pores inside soil aggregates or organic macromolecules, which are inaccessible to microorganisms. Degradation mediated by chemical reactions can be accelerated by enhanced adsorption due to catalytic effects of solid surfaces. Adsorption-catalyzed hydrolysis has been found for a number of pesticides including chlorotriazines (*46*).

Furthermore, only limited data are available for 12aβ-hydroxyrotenone, a more polar compound than rotenone but with other chemical characteristics that are rather unknown. It seems that the aging effect in rotenone degradation is more evident for 12aβ-hydroxyrotenone, considering its higher DT_{50}s and $K_{R\text{-}OH}$ d^{-1} values (**Table 3**) and its degradation curves (**Figures 4** and **5**). The existence of an aging effect in which hydrophobic organic chemicals become increasingly resistant to removal by water, organic solvent, or biological receptors with increased residence time is now widely documented, although the exact mechanisms remain subjected to debate (*11, 47, 48*). Factors such as contact time, temperature fluctuation, redox chemistry changes, wetting−drying cycles, or organic matter diagenesis can be important as contributing to the phenomenon. The present results clearly indicate that rotenone degradation in soil, which is strongly affected by several physicochemical parameters, is a chemical process markedly more complex than its photodegradation on soil surfaces.

LITERATURE CITED

(1) Cornejo, J.; Jamet, P.; Lobnik, F. Introduction. In *Pesticide/Soil Interactions. Some Current Research Methods*; Cornejo, J., Jamet, P., Coord.; INRA: Paris, France, 2000.

(2) Boesten, J. J. T. I.; van der Linden, A. M. A. Modelling the influence of sorption and transformation on pesticide leaching and persistence. *J. Environ. Qual.* **1991**, *20*, 425–435.

(3) Council Directive 91/414/EEC, 1991. (Annex IIA 7.1.1; Annex IIIA 9.1.1), The Plant Protection Directive, from 15 July, 1991. http://europa.eu.int.

(4) Guilhermino, L.; Celeste Lopes, M.; Carvalho, A. P.; Soares, A. M. V. M. Inhibition of acetylcholinesterase activity as effect criterion in acute tests with juvenile *Daphnia magna*. *Chemosphere* **1996**, *32*, 727–738.

(5) Hainzl, D.; Cole, L. M.; Casida, J. E. Mechanisms for selective toxicity of fipronil insecticide and its sulfone metabolite and desulfinyl photoproduct. *Chem. Res. Toxicol.* **1998**, *11*, 1529–1535.

(6) Reid, B. J.; Stokes, J. D.; Jones, K. C.; Semple, K. T. Biovailability of persistent organic pollutants in soils and sediments- a perspec-

tive on mechanisms, consequences and assessment. *Environ. Pollut.* **2000**, *108*, 103–112.
(7) Xing, B.; Pignatello, J. J. Dual-model sorption of low-polarity compound in glassy poly(vinyl chloride) and soil organic matter. *Environ. Sci. Technol.* **1997**, *31*, 792–799.
(8) Dec, J.; Bollag, J. M. Determination of covalent and non-covalent binding interations between xenobiotic chemicals and soil. *Soil Sci.* **1997**, *162*, 858–874.
(9) Gevao, B.; Semple, K. T.; Jones, K. C. Bound pesticide residues in soil- a review. *Environ. Pollut.* **2000**, *108*, 3–14.
(10) Brusseau, M. L.; Jessup, P. E.; Rao, S. C. Nonequlibrium sorption of organic chemicals: elucidation of rate-limiting processes. *Environ. Sci. Technol.* **1991**, *31*, 248–252.
(11) Pignatello, J. J.; Xing, B. Mechanisms of slow sorption of organic chemicals to natural particles. *Environ. Sci. Technol.* **1996**, *30*, 1–11.
(12) Cornelissen, G.; van Nort, P. C. M.; Govers, H. A. J. Mechanism of slow desorption of organic compounds from sediments: a study using model sorbents. *Environ. Sci. Technol.* **1998**, *32*, 3124–3131.
(13) Tomlin, C. D. S., Ed. *The pesticide Manual*, 12th ed.; BCPC: Farnham, U.K., 2000; pp 828.
(14) Crombie, L. Natural product chemistry and its part in the defence against insects and fungi in agriculture. *Pestic. Sci.* **1999**, *55*, 761–774.
(15) Yenesew, A.; Derese, S.; Midiwo, J. O.; Heydenrienreich, M.; Peter, M. G. Effect of rotenoids from the seeds of Millettia dura on larvae of *Aedes aegypti*. *Pest Manage. Sci.* **2003**, *59/10*, 1159–1161.
(16) Cabras, P.; Caboni, P.; Cabras, M.; Angioni, A.; Russo, M. Rotenone residues on olives and in olive oil. *J. Agric. Food Chem.* **2002**, *50*, 2576–2580.
(17) Cheng, H. M.; Yamamoto, I.; Casida, J. E. Rotenone Photodecomposition. *J. Agric. Food Chem.* **1972**, *20*, 850–856.
(18) Fukami, J. I.; Yamamoto, I.; Casida, J. E. Metabolism of rotenone in vitro by tissue homogenates from mammals and insects. *Science* **1967**, *155*, 713–716.
(19) Sariaslani, S. F.; Beale, M. J., Jr.; Rosazza, J. P. Oxidation of rotenone by Polyporus Anceps Laccase. *J. Nat. Prod.* **1984**, *47*, 692–697.
(20) Sariaslani, S. F.; Rosazza, J. P. Microbial Transformations of natural antitumor agents: Products of rotenone and dihydrorotenone transformation by *Cunninghamella blakesleeana*. *Appl. Environ. Microb.* **1983**, *45*, 616–621.
(21) Cavoski, I.; Caboni, P.; Sarais, G.; Cabras, P.; Miano, T. Photodegradation of rotenone in soils under environmental conditions. *J. Agric. Food Chem.* **2007**, *55*, 7069–7074.
(22) Augustijn-Beckers, P. W. M.; Hornsby, A. G.; Wauchope, R. D. The SCS/ARS/CES pesticide database for environmental decision-making II. *Rev. Environ. Contam. Toxicol.* **1994**, *137*, 1–29.
(23) EPIWIN (v. 3.12); U.S. EPA OPPT and Syracuse Research Corporation, 2004. http://www.epa.gov/opptintr/exposure/docs/episuitedl.htm.
(24) Hansch, C. D.; Hoekman, A.; Leo, L. O.; Zhang, P. Li. The expanding role of quantitative structure-activity relationship (QSAR) in toxicology. *Toxicol. Lett.* **1995**, *79*, 45–53.
(25) Decreto Ministeriale del 13 Settembre 1999. Metodi ufficiali di analisi chimica del suolo. Ministro per le Politiche Agricole. Gazz. Uff. Suppl. Ordin. no 248 del 21-10-1999.
(26) OECD Guidelines for the Testing of Chemicals Test No. 307: Aerobic and Anaerobic Transformation in Soils; Organisation for Economic Co-operation and Development: Paris, France, 2002.
(27) *FamilyGenetix, 2000*, ModelMaker 4.0; FamilyGenetix Ltf: Beaconsfield, Buckinghanshire, UK.
(28) FOCUS 2006. Guidance document on estimation persistence and degradation kinetics for environmental fate studies on pesticides in EU registration. Report of the FOCUS Work Group on Degradation Kinetics, EC Document Reference Sanco/10058/2005, Version 1.0 (final draft awaiting approval). European Commission, Brussels.
(29) Gustafson, D. I.; Holden, L. R. Non linear pesticide dissipation in soil: A new model based on spatial variability. *Environ. Sci. Technol.* **1990**, *24*, 1032–1038.
(30) Angioni, A.; Cabizza, M.; Melis, M.; Cabras, M.; Tuberoso, V. C.; Cabras, P. Effect of the epicuticular waxes of fruits and vegetables on the photodegradation of rotenone. *J. Agric. Food Chem.* **2004**, *52*, 3451–3455.
(31) Cabizza, M.; Angioni, A.; Melis, M.; Cabras, M.; Tuberoso, V. C.; Cabras, P. Rotenone and rotenoids in Cubè resins, formulations, and residues on olives. *J. Agric.Food Chem.* **2004**, *52*, 288–293.
(32) Ivie, G. W.; Casida, J. E. Sensitized photodecomposition and photosensitizer activity of pesticide chemicals exposed to sunlight on silica gel chromatoplates. *J.Agric. Food Chem.* **1971a**, *19*, 405–409.
(33) Ivie, G. W.; Casida, J. E. Photosensitizers for the accelerated degradation of chlorinated cyclodienes and other insecticide chemicals exposed to sunlight on bean leaves. *J. Agric. Food Chem.* **1971b**, *19*, 410–416.
(34) Environmental Protection Agency (EPA). *Environmental Fate and Ecological Risk Assessment for the Reregistration of Rotenone*; EPA-HQ-OPP-2005-0494-0016.phf; 2005; on-line.
(35) Hatzinger, P. B.; Alexander, M. Effect of ageing of chemicals in soil on their biodegradation and extractability. *Environ. Sci. Technol.* **1995**, *31*, 214–217.
(36) Pignatello, J. J. The measurement and interaction of sorption and sorption rates of organic compounds in a soil media. *Adv. Agron.* **2000**, *69*, 1–73.
(37) Ghosh, U.; Talley, J. W.; Luthy, R. G. Particle-scale investigation of PAH desorption kinetics and thermodynamics from sediment. *Environ. Sci. Technol.* **2001**, *35*, 3468–3475.
(38) Paraiba, L. C.; Spadotto, C. A. Soil temperature effect in calculating attenuation and retardation factors. *Chemosphere* **2002**, *48*, 905–912.
(39) Padilla, F.; Lafrance, P.; Robert, C.; Villeneuve, J. P. Modeling the transport and the fate of pesticides in the unsaturated zone considering temperature effects. *Ecol. Model.* **1988**, *44*, 73–88.
(40) Veeh, R. H.; Inskeep, W. P.; Camper, A. K. Soil depth and temperature effects on microbial degradation of 2, 4-D. *J. Environ. Qual.* **1996**, *25*, 5–12.
(41) Jurado-Exposito, M.; Walker, A. Degradation of isoproturon, propyzamide and alachlor in soil with constant and variable incubation conditions. *Weed Res.* **1998**, *38*, 309–318.
(42) Truman, C. C.; Leonard, R. A.; Davis, F. M. GLEAMSTC: a two-compartment model for simulating temperature and soil water content effects on pesticide losses. *Soil Sci.* **1998**, *163* (5), 362–373.
(43) Cavoski, I.; D'Orazio, V.; Miano, T. The Influence of Physico-Chemical Characteristics of Soils on Rotenone Mobility and Sorption Kinetics, The Fifth International Congress of the European Society of Soil Conservation, ESSC5, Palermo, Italia, 25−30 June, 2007; p 270.
(44) Kah, M.; Brown, C. D. Adsorption of ionisable pesticides in soils. *Rev. Environ. Contam. Toxicol.* **2006**, *188*, 149–218.
(45) Stotzky, G. Influence of Soil Mineral Colloids on Metabolic Processes, Growth, Adhesion, and Ecology of Microbes and Viruses. In *Interactions of Soil Minerals with Natural Organics and Microbes*; Huang, P. M., Schnitzer, M., Ed.; SSSA Spec. Publ., 17 SSSA, Madison, WI, 1986; pp 305−428.
(46) Hance, R. J. Influence of Adsorption on the Decomposition of Pesticides. In *Sorption and Transport Processes in Soil*; SCI Monogr. 37; Society of Chemical Industry: London, 1970; pp 92−104.
(47) Alexander, M. How toxic are toxic chemicals in soil? *Environ. Sci. Technol.* **1995**, *29*, 2713–2717.
(48) Luthy, R. G.; Aiken, G. R.; Brusseau, M. L.; Cunningham, S. D.; Gschwend, P. M.; Pignatello, J. J.; Reinhard, M.; Traina, S. J.; Weber, W. J., Jr.; Westall, J. C. Sequestration of hydrophobic organic contaminants by geosorbents. *Environ. Sci. Technol.* **1997**, *31*, 3341–3347.

Received for review May 9, 2008. Revised manuscript received July 7, 2008. Accepted July 8, 2008.

JF801461H